ndian J. Phys. 78 (7), 607-619 (2004)

AN INTERNATIONAL JOURNAL
IJP

On the diffraction model approach to cluster stripping nuclear reactions

Imad A Barghouthi[1]*, Mohammad M Abu-Samreh[1] and Nahida L Qumri[2]

[1]Department of Physics, College of Science and Technology, AL-Quds University, Abu-Deis, Jerusalem, PO Box 20002, via Israel

[2]114 William Lane, Oke Ridge, TN 37830, USA

E-mail : barghouthi2@yahoo.com

Received 26 December 2002, accepted 9 March 2004

Abstract In this study, the diffraction model is employed to study the cluster stripping nuclear reaction on the basis of the Regge-pole method A formula for the angular distribution is derived The angular distribution spectra for the cluster stripping nuclear reactions ^{40}Ca(^{3}He,p)^{42}Sc, ^{40}Ca (t,p)^{42}Ca and ^{54}Fe(t,p)^{56}Fe at various energies have been well reproduced with projectile energies varying between 10 MeV and 15 MeV The predicted theoretical results for the cluster stripping reactions ^{40}Ca (^{3}He,p)^{42}Sc with 10 MeV, 12 MeV and 15 MeV incident ^{3}He, ^{40}Ca (t,p)^{42}Ca with 10 1 MeV incident triton, and ^{54}Fe(t,p)^{56}Fe with 12 MeV incident triton were compared with the experimental data and good agreement was observed Also a comparison between the diffraction model prediction of the angular distribution values for the cluster stripping reaction ^{40}Ca(^{3}He,p)^{42}Sc at energy 12 MeV of ^{3}He and that of the distorted-wave Born approximation (DWBA) is implemented and a satisfactory agreement between the two methods has been attained

Keywords Cluster stripping nuclear reactions, diffraction model, Regge pole, angular distribution, DWBA model

PACS Nos. 24 10 Ht, 24.10 Eq

Introduction

Nuclear reactions model have played a vital role in revealing the structure of nuclides and have contributed to a deeper understanding of nuclear forces [1-14]. Detailed theories of nuclear reactions are patterned after the two principal models of nuclear structure, namely: the liquid-drop model for the compound-nucleus reaction and the shell-model for the direct reaction [13]. Theoretical considerations of nuclear reactions were aimed mostly on explaining the cross sections-dependence on energies and angles in terms of certain nuclear parameters such as nuclear radius and diffuseness.

The optical model was developed to cope with the complexities of nuclear reaction processes and to give a broad understanding of nuclear reactions encountered at bombarding energies above 10 MeV, including compound elastic scattering [3]. The complex term of the optical potential is introduced to take into account all possible reactions that fall in the absorption reaction categories and cause the removal of particles from the bombardment beam. This model has been particularly successful in explaining the total and the elastic cross sections of high energy nuclear reactions [3]. Besides, it predicts the broad resonances in cross sections as a function of energy.

The so-called plane-wave Born approximation (PWBA) was introduced to interpret the angular distribution of the cross section on a semi-quantitative basis. In the usual formulation of the PWBA calculations, the waves in the initial and final channels are generally generated by means of nuclear potential (optical potential) parameterization for elastic scattering. The deuteron stripping reactions, where the nucleon is supposed to be stripped off the incident deuteron by the nucleus at the nuclear radius, have been successfully studied in terms of this model [15,16]. However, the PWBA model calculation is usually sufficiently accurate to give the location of the first and perhaps the second maxima, it did not give a very accurate fit to the angular distribution and it was failed completely in predicting absolute cross-sections [17]. This is because the PWBA model ignores the effects of Coulomb potentials which, when a particle approaches close enough to have a reaction, leads to scattering and perhaps absorption of the particle [3]. This complication is taken into account in the distorted-wave Born approximation (DWBA), by treating the incident and emitted particles as particles moving under the influence of the nuclear potentials [17-19].

*Corresponding Author

The first phenomenological model suggested for the interpretation of the experimental results concerning the angular distribution of the direct nuclear reactions was the diffraction model [15]. According to this model, the nucleus is viewed as a 'black sphere' that absorbs certain incident partial waves. The calculation of the reflection coefficient requires parametrization of specific functions (in the form of Regge-type descriptions) for the continuation in the complex ℓ-plane [15,16]. A convenient parameterization is the Woods-Saxon type where the nuclear absorption can be expressed in terms of the reflection coefficient η_ℓ, whose parameterization is based on some nuclear parameters, namely: the nuclear radius and the diffuseness. In this case, the Regge-pole method can be employed to evaluate the partial-wave summation in the transition amplitude assuming a finite range for the reaction interaction response [16].

In this study, we advocate the diffraction model for describing the most common observed features of the angular distributions of the cluster stripping nuclear reactions. The choice of this model is motivated by several considerations. Firstly, the range of the diffraction phenomenon is wider than the nuclear radius. Thus, measurement of diffraction pattern as scattering distributions is of great importance in obtaining information about nuclear sizes and shapes. Secondly, the diffraction model takes care of essentially 'model-independent' aspects of nuclear scattering and reaction process [15]. Thirdly, theoretical considerations of nuclear reactions can be achieved using fewer nuclear parameters such as nuclear radius and diffuseness. Fourthly, calculation of the scattering matrix elements is based on the phase shift parameterization of the reflection coefficient η_ℓ, [20-22]. This model will be employed for studying the $T(\alpha,b)R$ cluster stripping nuclear reactions. The cornerstone based on obtaining a general formula for determining angular distributions starting from the transition matrix. The angular distributions of ^{40}Ca (^{3}He, p) ^{42}Sc, ^{40}Ca (t, p) ^{42}Ca and ^{54}Fe (t, p) ^{56}Fe cluster stripping nuclear reactions at various energies of incident particles (helium-3 and triton) will be examined. A comparison between the predicted values of the angular distribution obtained on the basis of the DWBA model and the present results of the angular distribution for the cluster stripping nuclear reaction ^{40}Ca (^{3}He, p) ^{42}Sc at 12 MeV energy of ^{3}He is included.

This paper is organized as follows: in Section 2, we derive the angular distribution formula. In Section 3, we present and discuss the results together with a comparison with the experimental data for the reaction ^{40}Ca (^{3}He, p) ^{42}Sc with projectile energies 10 MeV, 12 MeV and 15 MeV for incident ^{3}He; ^{40}Ca(t, p) ^{42}Ca at 10.1 MeV of incident triton; and ^{54}Fe (t,p) ^{56}Fe at 12 MeV of incident triton. In section 4, we present our conclusion. Finally in the appendix, we give a derivation of the angular distribution as calculated with the diffraction model with the stress on some mathematical details. Extension of this work to include other types of nuclear reactions is possible.

2. Theoretical considerations

There are several types of stripping nuclear reactions that have been introduced for studying the structure of single-nucleon and multi-nucleon states. Among one-nucleon stripping reactions are (d, p), (d, n), (t, d), (^{3}He, d), (α, ^{3}He), (α, t), (^{14}C, ^{15}O) *etc.* Many studies have been performed with two-nucleon stripping reactions like (t, p), (t, n), (^{3}He, p), (^{6}Li, α), (^{16}O, ^{14}N) *etc.*, three-nucleon stripping reaction like (α, p), four-nucleon stripping reactions like (^{6}Li, d) and (^{7}Li, t), five-nucleon stripping like (^{7}Li, d), *etc* [9-14]. A different type of reaction, which has been explained through the direct nuclear reaction processes is the deuteron cluster stripping nuclear reaction. In this type of reactions, an incident deuteron (^{2}H) is stripped off one of its component nucleons, which remain in the target nucleus and the remaining nucleon escapes [12].

One common feature of all direct reactions is the relationship between the angular momentum transferred in the reaction and the angular distribution of the emitted particles. Since these angular distributions are resulted from the superposition of waves emanating from the nucleus, interference effects leading to a diffraction-like pattern are expected [14]. Measurements of the differential cross section provide us with valuable information on the angular distribution of the reaction products. Frequently, a beam of incident particles may produce several types of reaction processes with a given target nucleus. By measuring the rate of each process separately, we can define the partial cross section for each reaction process and the sum of all partial cross sections is equal to the total cross section. In principle, the angular distribution can be put on a semi-quantitative basis by making use of the diffraction model [15].

We begin the diffraction model development of the cluster stripping nuclear reaction angular distributions by considering the general case problem. Let us consider the problem of deriving a formula for the differential cross section (or the angular distribution) as a function of incident particle's energy when bombarding a target nucleus T by an incident particle α in a nuclear reaction symbolized by the following reaction equation

$$\alpha + T \rightarrow R + b \quad \text{or} \quad T(\alpha, b)R\,.$$

In the above equation, we denote the lighter projectiles and fragments with α and b, and the target and final nucleus with T and R, respectively. The incident nucleus α will be assumed to form a bound state of b and c clusters, while R is assumed to form a bound state of the two clusters T and c. Symbolically this relation can be described as:

$$T + (c + b) \rightarrow (T + c) + b, \qquad (2)$$

where a cluster c is transferred to T and the parentheses denotes a bound state. The initial and final states of such reaction are schematically shown in Figure 1 (a).

As the incident nucleus approaches the target nucleus T, the target nucleus as seen by the incoming nucleus looks like a

region with a certain nuclear potential. The interaction of a beam of particles with the quantum potential well can be handled easily by means of the scattering theory [22]. The entrance and

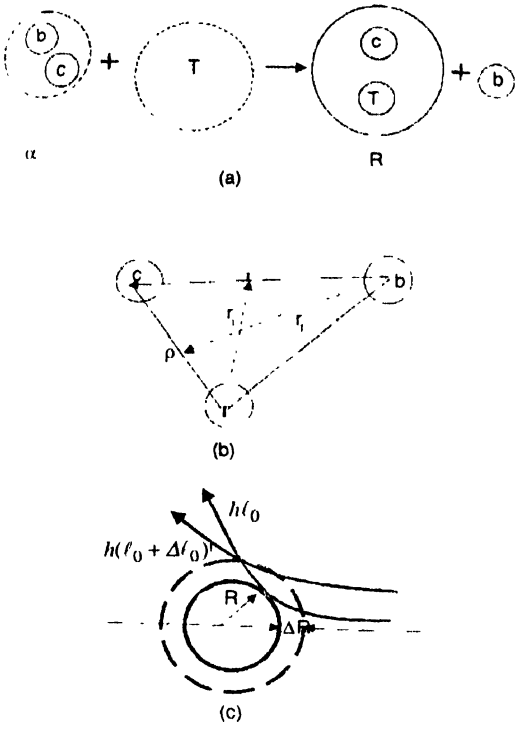

Figure 1. (a) Illustration of the cluster stripping nuclear reaction $T(\alpha, b)R$ (b) Vector diagram for the transfer process (c) A schematic diagram of a hypothetical nucleus with radius R and surface thickness $\Delta R = d$; $\Delta\ell$ is a measure of the number of partial waves over which the transition from zero to complete absorption occurs and it can be related to the nuclear surface diffuseness (d)

the exit channels can be described well in terms of potentials V_{bI}, V_{cT} and V_{bc}, respectively. The total Hamiltonians in the initial and final channels are given by :

$$H_i = H_i' + V_{bI} + V_{cT}\,, \tag{3}$$

$$H_f = H_f' + V_{bc} + V_{bT}\,, \tag{4}$$

where

$$H_i' = K_{\alpha I} + K_{bc} + V_{bc} \tag{5}$$

and

$$H_f' = K_{Rb} + K_{cT} + V_{cT}. \tag{6}$$

Here, K_{ij} (V_{ij}) is the relative kinetic energy (interaction potential) between the particles i and j.

For the cluster stripping nuclear reaction $T(\alpha, b)R$ in which a cluster c is transferred from α to T, the exact transition amplitude of the system when going from an initial state $(\alpha+T)$ at a given energy $E_{\alpha,T}$ to a final state $(b+R)$ is governed by the usual quantum mechanical matrix element [22]

$$T_{fi} = \left\langle \varphi_f \middle| V_f \middle| \psi_i^+ \right\rangle = \int \psi_i^{+*} V_f \varphi_f d\upsilon\,, \tag{7}$$

where T_{fi} is the matrix element between initial and final states, ψ_i^+ denotes a true stationary state of the complete Hamiltonian H_i describing an incident wave on the target nucleus T plus an outgoing scattered wave. Φ_f is the eigenstate of the Hamiltonian of the non-interacting states in the final channel *i.e.* H_f'. The interaction potential in the exit channel V_f can be written as:

$$V_f = V_{bc} + V_{bI}. \tag{8}$$

Thus, the time-independent Schrödinger wave equation can be written as

$$H_f'\Phi_f = E_f\Phi_f \Rightarrow \left[\frac{-\hbar^2}{2\mu}\nabla^2(r_f) + V_{cI}(\rho)\right]\Phi_f = E_f\Phi_f\,. \tag{9}$$

If the relative kinetic energy in the final channel is supposed to be much greater than the interaction potential *i.e.* $\frac{-\hbar^2}{2\mu}\nabla^2(r_f) >> V_{cT}(\rho)$, which is the condition for the Born approximation, the wave function of the final channel Φ_f can be written as :

$$\Phi_f = \varphi_R(\zeta)\,\varphi_b(\zeta)\,e^{ik_f r_f}. \tag{10}$$

Suppose that the cluster c position is closer to particle b than to the core of the cluster R, then the cluster will be considered within the external region of the core of T. By considering only the asymptotic behaviour of the outgoing spherical wave, which is given by a spherical Hankel function of the first kind $h_\lambda^{(1)}(kr)$ [23, 24], the wave function ψ_i^+ can be introduced as:

$$\psi_i^+ = \varphi_T(\xi)\varphi_\alpha(\xi)\quad e^{ik_i r_i}\quad 2\pi\sum_{\lambda m_\lambda} i^\lambda \eta_\lambda Y^*_{\lambda m_\lambda}\left(\hat{k}_i\right)$$

$$\times Y_{\lambda m_\lambda}(\hat{r}_i)\,h_\lambda^{(1)}(k_i r_i)\Big], \tag{11}$$

where φ_i is the internal wave function of the particle i ; $\rho - \frac{m_b}{\ldots}$ and $\frac{m_T}{m_c + m_T}|\rho - r$ are the relative position vectors in the initial and final channels. The vectors ρ and r are displayed in Figure 1(b). m_c, m_b and m_T are the masses of the transferred cluster, the outgoing particle and the target nucleus, respectively. ξ represents the internal coordinates that are independent of r, and ρ and $Y_{\ell m}(\theta, \varphi)$ are the spherical harmonic functions. k_i and k_f are the relative wave vectors in the initial and final channels, respectively. The reflection coefficients parameters η_λ, are expressed in terms of the convenient Wood-Saxon form as:

$$\eta_\ell = \left\{1 + \exp\quad^{(\ell-\ell_0)}\right. \tag{12}$$

where ℓ_0 is the cut-off angular momentum and Δ is the diffuseness parameter. The form of reflection parameter as introduced in eq. (12) implies that the transition of η_ℓ from zero to unity is expected to take place gradually and is extended over a wide range of ℓ values of the transition width Δ. This is illustrated in Figure 1(c) in the vicinity of ℓ_0 in order to take into account the nuclear surface thickness.

Let us now expand the wave functions of the nuclei α and R in terms of the different states of b and T, respectively, times the wave function of the cluster c. The results are

$$\varphi_\alpha = \sum \begin{Bmatrix} S_c & \mu_c & LM \\ J_c & M_c & \end{Bmatrix} S\{\alpha,c,b\} \left[(S_c \mu_c, LM/J_c M_c) \times (J_c M_c, S_b \mu_b | S_\alpha \mu_\alpha) \right] \varphi_b(\xi)\, \varphi_c(\xi)\, R_{LM}(r), \quad (13)$$

$$\varphi_R = \sum \begin{Bmatrix} S_c & \mu_c & \ell M \\ j_c & m_c & \end{Bmatrix} S\{R,T,c\} \left[(S_c \mu_c, \ell m/J_c m_c) \times (j_c m_c, S_T \mu_T | S_R \mu_R) \right] \varphi_c(\xi)\, \varphi_T(\xi)\, R_{\ell m}(\rho). \quad (14)$$

Here, S and μ are the spin and its projection, respectively; while LM and ℓm are the relative angular momentum and its projection in the incident and final channels. Both $J_c M_c$ and $j_c m_c$ represent the total angular momentum of the cluster c in the projectile and the residual nuclides. The symbol R is used to represent the relative wave function and the bracket denotes the relevant Clebsch-Gordan coefficients. Now, using eqs. (8), (10), (11), (13), and (14), the transition amplitude in eq. (7) becomes

$$T_{fi} = \sum \begin{Bmatrix} S_c & \mu_c, & \ell m, & LM \\ J_c & m_c, & J_c & M_c \end{Bmatrix} S\{R,T,c\}\, S\{\alpha,c,b\} \times (S_c \mu_c, \ell m | j_c m_c)(j_c m_c, S_T \mu_T | S_R \mu_R)(S_c \mu_c, LM | J_c M_c) \times (J_c M_c, S_b \mu_b | S_\alpha \mu_\alpha) \Big\langle \varphi_c(\xi)\, \varphi_T(\xi)\, R_{\ell m}(\rho) \varphi_b(\xi) e^{ik_f r_f} V_f | \varphi_b(\xi) \varphi_c(\xi) R_{LM}(r) \varphi_T(\xi) e^{ik_i r_i} + 2\pi \sum i^\lambda \eta_\lambda Y^*_{\lambda m_\lambda}(\hat{k}_i)\, Y_{\lambda m_\lambda}(\hat{r}_i)\, h^{(1)}_\lambda(k_i r_i) \Big\rangle. \quad (15)$$

The vector diagrams of k_f, k_i and $k'f$ are displayed in Figure 2 (a); while the complex plane for calculating the residues is shown in Figure 2 (b) (see Appendix). By making use of the normalization condition

$$\left\langle \varphi_c(\xi) \varphi_T(\xi) \varphi_b(\xi) | \varphi_b(\xi) \varphi_c(\xi) \varphi_T(\xi) \right\rangle = 1. \quad (16)$$

Therefore, the transition amplitude can be rewritten as :

$$T_{fi} = C[I_1 + I_2], \quad (17)$$

where

$$C = \sum \begin{Bmatrix} S_c & \mu_c, & LM, & \ell m \\ J_c & M_c, & j_c & m_c \end{Bmatrix} S^*\{R,T,c\}\, S\{\alpha,c,b\} \times (S_c \mu_c, \ell m\ j_c m_c)(j_c m_c, S_T \mu_T\ S_R \mu_R)(S_c \mu_c, LM\ J_c M_c) \times (J_c M_c, S_b \mu_b\ S_\alpha \mu_\alpha),$$

$$I_1 = R_{\ell m}(\rho) e^{ik_f \cdot r_f} V_f R_{LM}(r) e^{ik_i \cdot r_i} \quad (18)$$

and

$$I_2 = 2\pi e^{ik_f r_f} R_{\ell m}(\rho) V_f R_{LM}(r) \sum_{\lambda m_\lambda} i^\lambda \eta_\lambda Y^*_{\lambda m_\lambda} \times (\hat{k}_i) Y_{\lambda m_\lambda}(\hat{r}_i) h^{(1)}_\lambda(k_i r_i). \quad (19)$$

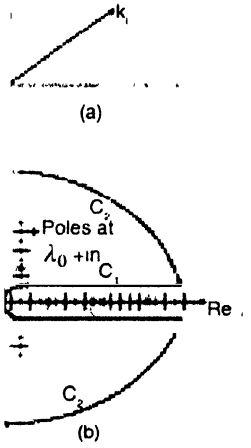

Figure 2. (a) Schematic representation of the quantization axis k_f (b) The contour integration in the ν-complex plane together with the Regge poles positions of η_ν as given by equation (A 49)

Since V_{bc} corresponds to a bound state in the entrance channel, one may expect that the contribution of V_{bc} to be much greater than that of V_{bT}, and hence the latter term in eq. (8) can be neglected with respect to the former [25]. Using eq (17), the angular distribution can be introduced as:

$$\frac{d\sigma}{d\Omega} \propto T_{fi}^2 \propto I_1 + I_2^2,$$

where I_1 and I_2 are given by the following expressions (see Appendix for derivation):

$$I_1 = (4\pi)^{3/2} N_0 V_0 \sum_{\ell m} (i)^\ell N_\ell Y^*_{\ell m}(\hat{Q}) \frac{(2Q)^\ell \Gamma(\ell+1)}{(Q^2+\gamma^2)^{\ell+1}(q^2+\beta^2)} \quad (20)$$

and

$$I_2 = 16\pi^2 \Delta \sum_{\ell m} (-1)^m N_0 V_0 N_\ell \frac{\Gamma(\ell+2)}{\beta^2 \gamma^{\ell+2}} j_{\ell 0}(k'_f R_{cT})$$

$$\times J_{\ell 0}(k_i R_{iT}) j_{\ell 0}(k_f R_{bc}) h_{\ell 0}^{(1)} \frac{m_c}{m_c + m_b} k_i R_{bc}$$

$$\times \frac{(4\lambda_0^2 + 2\pi^2\Delta^2)^{5/2}}{(2\lambda_0)^{5/2}\sqrt{\sin\vartheta}} \sin\left[\left(\lambda_0 + \frac{1}{2}\right)\vartheta - \frac{\pi}{4} + \frac{5\pi\Delta}{2\lambda_0}\right] e^{-\pi\Delta\vartheta}. \quad (23)$$

The required angular distribution is generally proportional to differential cross section of cluster stripping reactions. Thus

$$\text{angular distribution} \propto \frac{d\sigma}{d\Omega} \propto \quad :|I_1 + I_2|^2. \quad (24)$$

The above equation is the one to be used in the present study.

3. Results and discussion

Theoretically, the contribution of the stripping cluster nuclear reactions to the various cross sections spectra (or angular distributions) is presented by the functional form of eq. (24). In the calculations, only the case when the transferred cluster is in a relative s-state is considered. A careful choice of integration variables and nuclear reaction parameters facilitates the theoretical calculations. Two open parameters are involved in the calculations, namely, the nuclear radius R and surface diffuseness parameter Δ. The corresponding angular distribution results for the cluster stripping reactions ^{40}Ca (^{3}He, p) ^{42}Sc, ^{40}Ca(t, p) ^{42}Ca, and ^{54}Fe(t, p) ^{56}Fe at different energies of incident particles and for different nuclear radii and diffuseness parameters are included. Accordingly, for each cluster stripping nuclear reaction, families of curves can be obtained by varying either the nuclear radius parameter or the diffuseness parameter. The obtained results are displayed as a function of the center-of-mass scattering angle ranges between $0^0 < \theta_{c.m} < 160^0$. Plots of this type are useful for the comparison purposes of the experimental values with the calculated theoretical values, in order to test the success of the model.

The predicted theoretical results of angular distribution functions according to eq. (24) of the ground-state protons for the cluster stripping nuclear reaction ^{40}Ca(^{3}He,p) ^{42}Sc with projectile energies 10 MeV, 12 MeV and 15 MeV of incident ^{3}He; ^{40}Ca(t, p) ^{42}Ca at 10.1 MeV of incident t; and ^{54}Fe(t, p) ^{56}Fe at 12 MeV of incident t for certain selective best-fit parameters together with the experimental data are displayed in Figures 3-6. The calculated values of the angular distributions of the ground-state proton for the cluster stripping nuclear reaction ^{40}Ca(^{3}He,p)^{42}Sc are exhibited in Figures, 3-5. In Figure 3(a), shown the predicted diffraction model results of the angular distribution for this reaction at energy of 10 MeV for incident ^{3}He and diffuseness parameter of 0.40 but using different radius parameters of 6.28, 7.18 and 8.08 fm together with experimental data taken from Ref. [26]. Shown in Figure 3(b) the predicted results for the reaction with the same energy for incident ^{3}He but using different radius parameter of 6.28 fm and different diffuseness parameters of 0.30, 0.40 and 0.50 together with the experimental data taken from Ref. [26]. Figure 3(c) displays the predicted results obtained by using the best-fit parameters R = 6.28 fm and Δ = 0.4 together with the experimental data taken from Ref. [26] for the same reaction.

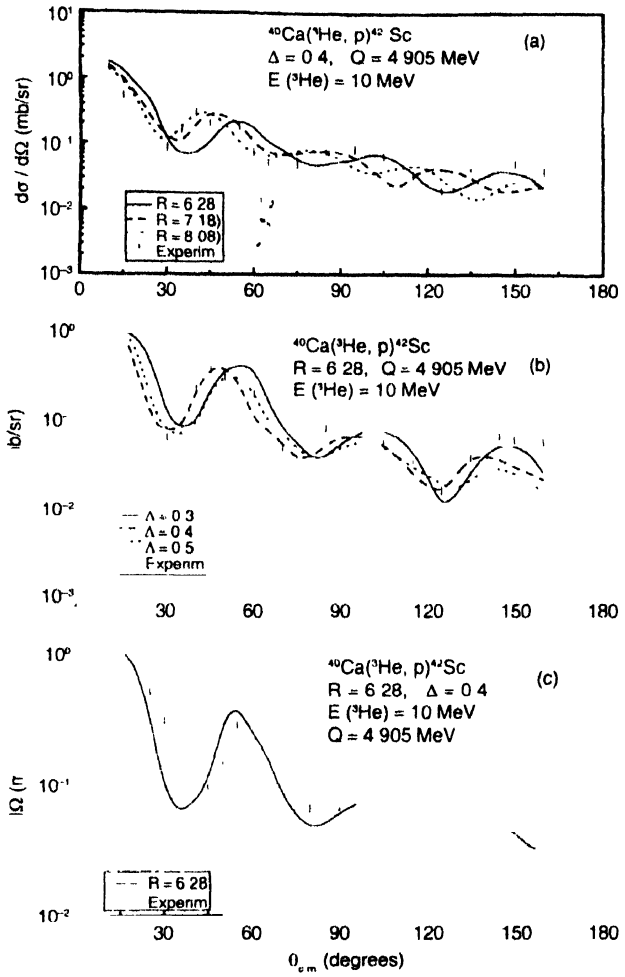

Figure 3. The results of angular distributions using the diffraction model together with the experimental data taken from Ref [26] as a function of the scattering angle $\theta_{c.m}$ of the ground-state protons for various cluster stripping processes in the reaction ^{40}Ca (^{3}He,p)^{42}Sc at E_{lab} = 10 and (a) R = 6 28, 7 18 and 8 08 fm and Δ = 0 40 (b) Δ = 0 30, 0 40 and 0 50 and R = 6 28 fm (c) best-fit parameters are R = 6 28 fm and Δ = 0.40

Shown in Figure 4 the angular distribution of the ground-state protons for the same reaction ^{40}Ca (^{3}He,p)^{42}Sc, with 12 MeV incident ^{3}He for different radius parameters and different diffuseness parameter together with the experimental data taken from Ref. [26] and the best-fit parameters (R = 6.80 fm and Δ = 0.4) curves. In Figure 4(a), values of the angular distribution are obtained by making use of the radius parameter values of 6.80, 6.56, 5.20, and 4.91 fm together with the diffuseness parameter value of 0.40. In obtaining the results of the distribution function exhibited in Figure 4(b), we have taken the

radius parameter value to be 6.80 fm and the diffuseness parameter values are taken to be 0.35, 0.40, 0.45 and 0.50. In Figure 4(c) the results for best-fit parameters are plotted together with the expeimental data. Similarly, in Figure 5 we have displayed the results of this reaction with 15 MeV incident ^{3}He but with different parameters together with the experimental data taken from Ref. [26]. In Figure 5(a), we have plotted the angular distributions obtained using a diffuseness parameter of 0.40 and radius parameters of 4.41 and 5.15 fm together with the experimental data. Figure 5(b) displays the angular distributions for radius parameter of 4.41 fm and diffuseness parameters of 0.30, 0.40 and 0.50 together with the experimental data. Last, shown in Figure 5(c) are the angular distribution results attained by using the best-fit parameters R = 4.41 fm and $\Delta = 0.3$ together with the experimental data.

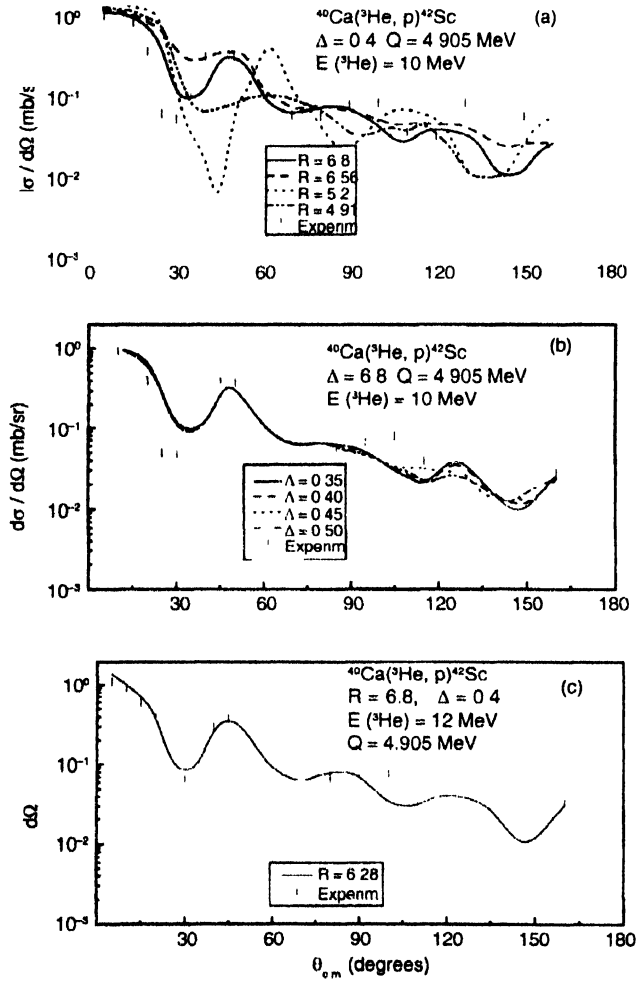

Figure 4. The results of angular distributions using the diffraction model together with the experimental data taken from Ref. [26] as a function of the scattering angle $\theta_{c.m}$ of the ground-state protons for various cluster stripping processes in the reaction ^{40}Ca (^{3}He, p)^{42}Sc at $E_{^3He} = 12$ and (a) R = 6.80, 6.56, 5.20 and 4.91 fm and $\Delta = 0.40$ (b) $\Delta = 0.35$, 0 40, 0.45 and 0.50 and R = 6.80 fm. (c) best-fit parameters are R = 6.80 fm and $\Delta = 0.40$.

It can be seen from the Figures 3, 4 and 5 that the diffraction model approach can predict well the general behaviour of the angular distribution. Furthermore, the calculated angular distribution values using the best-fit parameters are similar to that of the experimental data. In particular, at small angles, it reveals that both experimental and theoretical values of angular

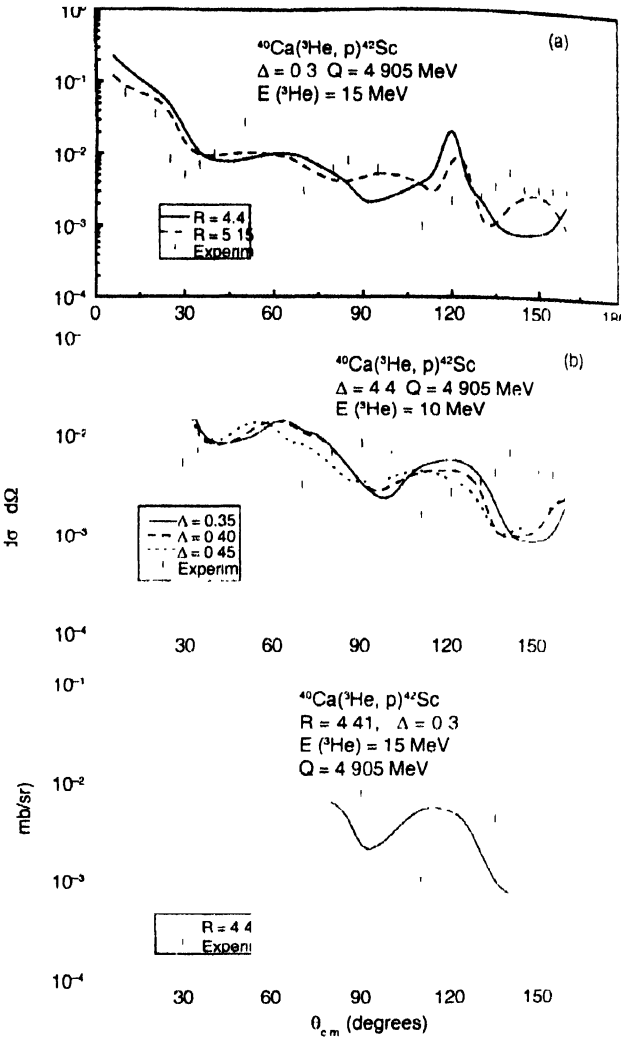

Figure 5. The results of angular distributions using the diffraction model together with the experimental data taken from Ref. [26] as a function of the scattering angle $\theta_{c.m}$ of the ground-state protons for various cluster stripping processes in the reaction ^{40}Ca (^{3}He,p)^{42}Sc at $E_{^3He} = 15$ MeV and (a) R = 4 41 and 5 15 fm and $\Delta = 0.30$ (b) $\Delta = 0$ 30, 0 40 and 0 50 and R = 4 41 fm. (c) best-fit parameters are R = 4 41 fm and $\Delta = 0$ 30

distributions are too large. After that the angular distribution values continue to decrease in the center-of mass angle range $0^0 < \theta_{c.m.} < 160^0$. An oscillation of maximum and minimum and a persistence of the prominent feature of these curves has been observed. The diffraction-like behaviour starts to show up at large angles beyond 30°. The observed diffraction pattern in the differential cross section plots may be attributed to the interference from opposite sides of the nucleus [4]. The diffraction model interpretation of the observed general trend of the angular distribution is as follows: Interference between the diffracted waves resulted in the appearance of the maximum and minimum of the distribution functions. The corresponding

resonating partial wave is large in the surrounding of potential dip region, consequently the overlapping probability of nuclides and their surface regions also increased. Therefore, an increased absorption at resonance energy, leads to the dip-peak structure of the reflection coefficient [26-28] indicating the presence of the Regge-pole in $|\eta_\lambda|$ [29]. Thus, a decrease in the distribution functions will be produced [14]. This approach might be inapplicable at high energies (> 100 MeV) where larger angular momenta are involved and the dips in the effective potential vanish [30]. One may notice in Figures, 3, 4 and 5 that the general drop-off trend of the angular distribution functions is dependent on the radius parameter. With a larger radius parameter, the angular distribution of diffraction patterns, the maximum as well as the minimum peaks, are shifted toward the small angles, while their shapes remain similar. These observed regular features are similar for all predicted angular distribution values using the diffraction model.

Similar angular distribution results were obtained for both ^{40}Ca(t,p)^{42}Ca and ^{54}Fe(t,p)^{56}Fe nuclear stripping reactions with 10.1 MeV and 12 MeV incident triton, respectively. The angular distribution predicted results using the selected best-fit parameters for both reactions together with the experimental data taken from Ref. [26,30] were exhibited in Figure 6. The general remarks made for reaction ^{40}Ca(^{3}He,p)^{42}Sc still remain valid for the other reactions, that is, the angular distribution results follow the general trend of the experimental data.

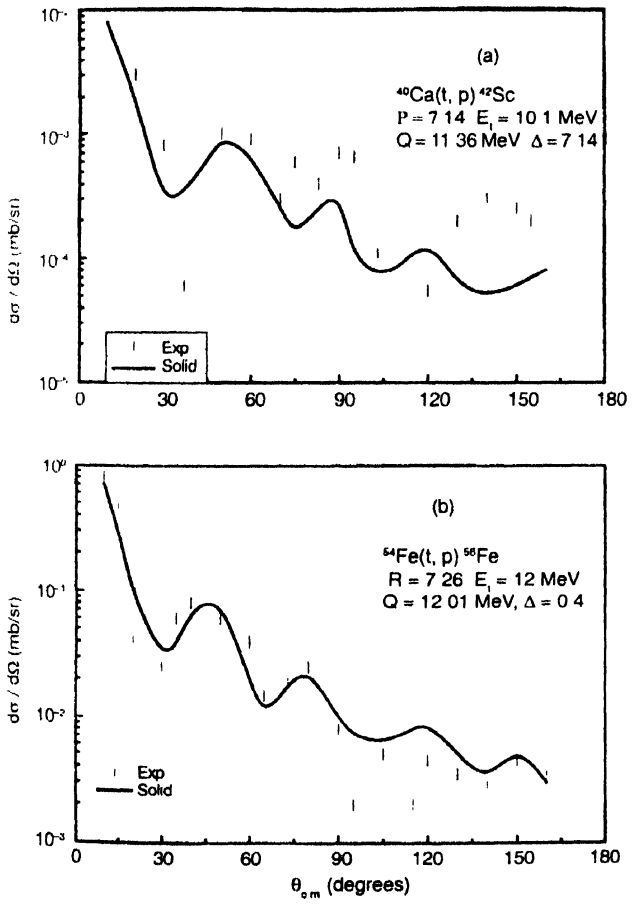

Figure 6. The angular distribution for the ground-state reactions for various cluster stripping processes in the reaction, (a) ^{40}Ca (t , p)^{42}Ca, at E_t = 10.1 MeV, using the best-fit parameters of R = 7.14 fm and Δ = 0.4 The experimental points are taken from Ref. [31]. (b) ^{54}Fe (t, p)^{56}Fe at E_t = 12 MeV, using the best-fit parameters of R = 7.26 fm and Δ = 0.4. The experimental points are taken from Ref. [27].

After testing the validity of the diffraction model against the experimental data for the cluster stripping reactions ^{40}Ca (^{3}He,p)^{42}Sc, ^{40}Ca (t, p)^{42}Ca and ^{54}Fe(t,p)^{56}Fe, a comparison between the present results of the angular distributions to those obtained in the DWBA calculations for the cluster stripping reaction ^{40}Ca (^{3}He, p) ^{42}Sc has been made. For this purpose, the angular distributions for the reaction ^{40}Ca (^{3}He,p)^{42}Sc, with 12 MeV incident ^{3}He and of best-fit parameters R = 4.91 fm and Δ = 0.40, as predicted by the diffraction model approach and that calculated by the DWBA approach taken from Ref. [25] are plotted in Figure 7. The dashed curve in Figure 7 corresponds to the predicted diffraction model results using the best-fit parameters R =7 26 fm and Δ = 0.4 and the solid curve represents the DWBA predicted results. It is clear from the figure that a satisfactory agreement between the predicted results of the two approaches has been attained.

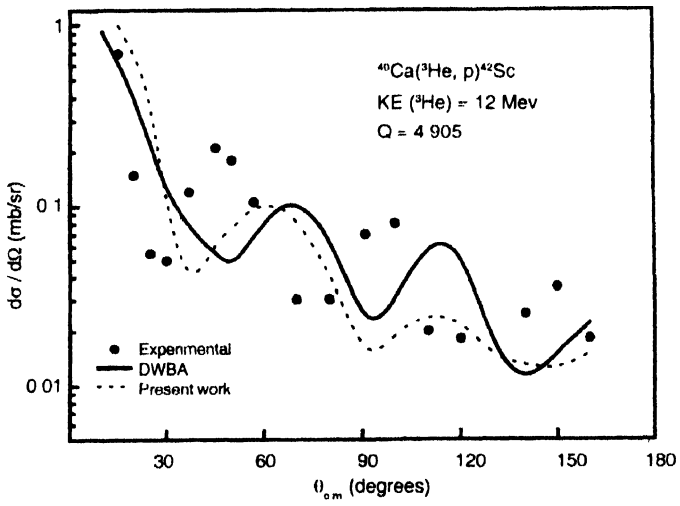

Figure 7. Comparison between the angular distributions of the reaction ^{40}Ca (3He,p)^{42}Sc, at E_{lab} = 12 MeV, as predicted in the present work (dashed line) with DWBA calculations [26] (solid line)

4. Conclusion

The diffraction model has been employed successfully to obtain an expression of the angular distributions of the cluster stripping nuclear reaction $T(a,b)R$. The experimental data of the angular distributions spectra for the reactions ^{40}Ca(^{3}He,p)^{42}Sc, ^{40}Ca (t,p)^{42}Ca and ^{54}Fe(t,p)^{56}Fe at various energies have been well reproduced at an incident particle's energies varying between 10 MeV and 15 MeV. The predicted theoretical results were found to be in agreement with the experimental data. A comparison between the diffraction model predicted values of the angular

distribution for the reaction ^{40}Ca (^{3}He,p)^{42}Sc with 12 MeV incident ^{3}He and the calculated values using DWBA reveals a satisfactory agreement between the two methods.

In conclusion, the low energy (0.1–50 MeV) cluster stripping nuclear reactions can be adequately explained in terms of the diffraction model. Besides, the diffraction model approach is capable of reproducing the main features of nuclear reactions differential cross sections properly. Extension of this work to include contributions other than s-state is recommended to test the validity of the diffraction model for attaining the general features of high energy (> 100 MeV) nuclear reactions.

References

[1] G R Satchler *Introduction to Nuclear Reactions*, 2nd edn (London : MacMillan) (1990)

[2] N A Dyson *An introduction to Nuclear Physics, with applications in Medicine and Biology* (New York : John Wiley) (1981)

[3] N A Jelley *Fundamentals of Nuclear Physics* (Cambridge : Cambridge University Press) (1990)

[4] K S Krane *Introductory Nuclear Physics* (New York John Wiley) (1988)

[5] E J Burge *Atomic Nuclei and their Particles*, 2nd edn (Oxford Clarendon Press) (1988)

[6] U Stiegler *Phys. Rep* **277** 1 (1996)

[7] S Rombouts and K Heyde *Phys Rev Lett.* **80** 885 (1998)

[8] M S EL-Nagdy *Mod. Phys. Letts* **A16** 985 (2001)

[9] M EL-Nadi, M S EL-Nagdy, N Ali-Mossa, A Abdesalam, A M bdalla and A A Hamed *J Phys.* **G25** 1169 (1999)

[10] K Heyde *Basic Ideas and Concepts in Nuclear Physics : An Introductory Approach*, 2nd edn (Bristol Institute of Physics Publishing) (1999)

[11] M EL-Nadi, M S EL-Nagdy, N Ali-Mossa, A Abdesalam, A M bdalla and S M Abdel-Halim *J. Phys.* **G28** 1251 (2002)

[12] W Tobocman *Theory of Direct Nuclear Reactions* (London. Oxford Press) (1963)

[13] B L Cohen *Concepts of Nuclear Physics* (New Delhi McGraw-Hill) (1971)

[14] W E Frahn *Diffractive Processes in Nuclear Physics* (Oxford Clarendon Press) (1985)

[15] W E Frahn and R H Venter *Ann. Phys.* **24** 243 (1963)

[16] M El-Nadi *Phys. Rev.* **120** 1360 (1960)

[17] G Delic *Nucl. Phys.* **A158** 117 (1971)

[18] W E Frahn and K E Rehm *Phys. Rep* **37c** 1 (1978)

[19] W E Frahn and M S Hassin *Nucl. Phys.* **A346** 237 (1980)

[20] R J Slobodrian, C Riox, R Roy, H E Conzett, P Von Rossen and F Hinterberger *Phys Rev Lett.* **47** 1803 (1981)

[21] P M Lewis, O Karban, J M Barnwell, J D Brown, P V Drumm J M Nelson and S Roman *Nucl. Phys.* **A404** 205 (1983)

[22] D J Griffiths *Introduction to Quantum Mechanics* (New Jersey Prentice-Hall) (1995)

[23] G Arfken *Mathematical Methods for Physicists*, 4th edn (New York . Academic Press) (1996)

[24] G N Watson *Proc. Roy Soc.* **A95** 83 (1918)

[25] M El-Nadi, T H Rihan and O Zahni *Nucl. Phys* **82** 417 (1966)

[26] R W Zurmühle, C M Fou and L W Swenson *Nucl Phys* **80** 25 (1966)

[27] R M Drisko and F Rybicki *Phys. Rev. Letts.* **16** 275 (1966)

[28] H Voit and H D Helb *Nucl Phys* **A204** 196 (1973)

[29] T Tamura and H H Wolter *Phys Rev* **C6** 1967 (1972)

[30] D A Saloner and C Toepffer *Nucl Phys* **A283** 131 (1977)

[31] B F Baym and N M Hintz *Phys Rev* **172** 1113 (1968)

[32] F B Morinigo *Phys. Rev* **134** B1243 (1964)

[33] J Spani and K Oldham *An Atlas of Functions* (New York Hemisphere publication) 521 (1987)

[34] M K Pal *Theory of the nuclear structure* (New Delhi Affiliated East-West Press Private Ltd) (1982)

[35] F B Morinigo *Nucl Phys.* 77 289 (1966)

[36] A R Edmonds *Angular Momentum in Quantum Mechanics* (New York· Princeton University Press) (1974)

[37] J Høgaasen *Nucl Phys.* **A90** 261 (1967)

[38] W E Frahn and M A Sharaf *Nucl Phys* **A133** 593 (1969)

[39] D M Brink and N Rowley *Nucl. Phys* **A219** 79 (1974)

[40] G R Satchler *Rev Mod. Phys.* **50** (1978)

Appendix : Derivation of the angular distribution for cluster stripping nuclear reactions

In this appendix, we shall give a complete derivation of the angular distribution by evaluating both I_1 and I_2 terms. Let us first consider the first term in the transition amplitude expressed in eq. (19), *i.e.*, I_1. Substituting the given values of r_f and r_i, we obtain

$$I_1 = \Bigg\langle R_{\ell m}(\rho) e^{ik_f\left(\frac{m_T}{m_c+m_f}\right)\rho} e^{-ik_f\cdot r} |V_{bc}| R_{LM}(r) e^{-ik_i\cdot\rho} \times e^{-ik_i\left(\frac{m_b}{m_b+m_c}\right)r} \Bigg\rangle$$

$$= \int R^*_{\ell m}(\rho) e^{i\left(k_i - \frac{m_T}{m_c+m_T}k_f\right)\rho} V_{bc}(r) e^{i\left(k_f - \frac{m_b}{m_b+m_c}k_i\right)} \times R_{LM}(r)\, dr\, d\rho . \quad (A.1)$$

By introducing the following coordinates :

$$Q = k_i - \frac{m_T}{m_c+m_T} k_f , \quad (A.2)$$

$$q = k_f - \frac{m_b}{m_b+m_c} k_i , \quad (A.3)$$

eq. (A.1) can be rewritten as:

$$I_1 = \int u^*_\ell(\rho)\, e^{iQ\cdot\rho} Y^*_{\ell m}(\hat{\rho})\, d\rho \int e^{iq\cdot r} V_{bc}(r) u_L(r) Y_{LM}(\hat{r}) dr. \quad (A.4)$$

In eq. (A.4), we have expressed $R_{\ell m}(\rho)$ and $R_{LM}(r)$ in terms of spherical harmonics using

$$R^*_{\ell m}(\rho) = u^*_\ell(\rho)\, Y^*_{\ell m}(\hat{\rho}), \tag{A.5}$$

$$R_{LM}(r) = U_L(r)^I\, Y_{LM}(\hat{r}). \tag{A.6}$$

Since the nuclear states are eigenstates of angular momentum, it is useful to expand the plane wave in spherical harmonics using the following expansions [22]:

$$e^{ik\,r} = 4\pi \sum_{\nu m_\nu} i^\nu j_\nu(kr)\, Y^*_{\nu m_\nu}(\hat{k})\, Y_{\nu m_\nu}(\hat{r}),$$

$$Y_{\nu' m_{\nu'}}(\hat{r}) = (-)^m \nu' Y^*_{\nu' -m_{\nu'}}(\hat{r}). \tag{A.7}$$

q (A.4) can be rewritten as:

$$= (4\pi)^2 \sum_{\nu m_\nu} \sum_{\nu' m_{\nu'}} (i)^\nu (i)^{\nu'} (-)^{m_{\nu'}}\, Y^*_{\nu m_\nu}(\hat{Q}) Y^*_{\nu' m_{\nu'}}(\hat{q})$$

$$\times \int Y_{\nu m_\nu}(\hat{\rho}) Y^*_{\ell m}(\hat{\rho}) d\Omega_\rho \int Y^*_{\nu' -m_{\nu'}}(\hat{r}) Y_{LM}(\hat{r})\, d\Omega,$$

$$\times \int u^*(\rho) j_\nu(Q_\rho)\, \rho^2 d\rho \int j_{\nu'}(qr) V_{b\iota}(r) u_L(r) r^2 dr,$$

$$= (4\pi)^2 \sum_{\ell m} \sum_{LM} (i)^\ell (i)^I (-)^{-M} Y^*_{\ell m}(\hat{Q}) Y^*_{L,M}(\hat{q}) \times \tau_1, \tag{A.8}$$

here

$$\tau_1 = \int u^*_\ell(\rho) j_\ell(Q_\rho)\, \rho^2 d\rho \int j_L(qr)\, V_{b\iota}(r)\, U_L(r) r^2 dr \tag{A.9}$$

nd $J_n(x)$ is the spherical Bessel function which is related with e ordinary Bessel function by the relation [23]:

$$J_n(x) = \sqrt{\frac{\pi}{2x}} J_{n+\frac{1}{2}}(x). \tag{A.10}$$

Taking $u_\ell(\rho)$ to be the Morinigo wave functions whose neral form can be written as [31]:

$$u_\ell(\rho) = N_\ell e^{-\gamma\rho} \rho^{\ell-1}, \tag{A.11}$$

here $N_\ell = \sqrt{\dfrac{(2\gamma)^{2\ell-1}}{\Gamma(2\ell-1)}}$ is the normalization constant of the ave function,

$= \sqrt{\dfrac{2\mu_{cT}\varepsilon_{cT}}{\hbar^2}}$, $\mu_{cT} = \dfrac{m_c m_T}{m_c + m_T}$, ε_{cT} is the binding energy the system, $(c+T) \equiv R$, and Γ is the gamma function. erefore, for the first integral of eq. (A.9), we may obtain an pression of the form:

$$\int u^*_\ell(\rho) j_\ell(Q_\rho)\, \rho^2 d\rho = N_\ell (2Q)^\ell \frac{\Gamma(\ell+1)}{\left(\gamma^2+Q^2\right)^{\ell+1}}. \tag{A.12}$$

The integral in eq. (A.12) have been evaluated using the following standard integral [32, 33]:

$$\int e^{-\gamma\rho} J_\nu(Q\rho)\, \rho^\nu d\rho = \frac{(2Q)^\nu \Gamma\left(\nu+\frac{1}{2}\right)}{\left(Q^2+\gamma^2\right)^{\nu+\frac{1}{2}} \sqrt{\pi}}. \tag{A.13}$$

In evaluating the second integral of eq. (A.9), we have assumed that the projectile is in a relative S-state, where $L = M = 0$ and the nuclear potential of Hulthen type. A pure central potential of Hülthen form yields an analytic solution of the S-state of Schrödinger wave equation [34]. If the Hülthen forms were chosen [35] for both the wave function $u_0(r)$ and the potential $V_{b\iota}$, one may write

$$u_0(r) = N_0 \left(\frac{e^{-\alpha r} - e^{-\beta r}}{r} \right), \tag{A.14}$$

$$V_{b\iota}(r) = V_0 \left| \frac{e^{-\beta r}}{e^{-\alpha r} - e^{-\beta r}} \right|, \tag{A.15}$$

where $N_0 = \dfrac{[\alpha\,\beta(\alpha+\beta)]}{\beta-\alpha} \dfrac{}{2\pi}$ is the normalization constant of the wave function, $\beta = 7\alpha$[25], $\alpha = \sqrt{\dfrac{2\mu_{cb}\varepsilon_{cb}}{\hbar^2}}$, $\mu_{cb} = \dfrac{m_b m_c}{m_b + m_c}$, $V_0 = \dfrac{-\hbar^2}{2\mu_{cb}}\left(\beta^2 - \alpha^2\right)$, and ε_{cb} binding energy of the system $(b+c) \equiv \alpha$, then the second integral of eq. (A.9) is given by

$$\int_0^\infty j_L(qr)\, V_{b\iota}(r)\, U_L(r)\, r^2 dr = N_0 V_0 \frac{1}{\left(q^2+\beta^2\right)}, \tag{A.16}$$

where eqs. (A.10) and (A.12) have been used. Using eqs. (A.8), (A.12) and (A.16) we get:

$$I_1 = (4\pi)^{3/2} N_0 V_0 \sum_{\ell m} (i)^\ell N_\ell Y^*_{\ell m}(\hat{Q}) \frac{(2Q)^\ell \Gamma(\ell+1)}{\left(Q^2+\gamma^2\right)^{\ell+1}\left(q^2+\beta^2\right)}. \tag{A.17}$$

The second part of the transition amplitude, *i.e.* I_2 can be evaluated as follows:

We shall first expand the spherical harmonics and the spherical Hankel function appearing in I_2 to obtain r and ρ in separate function as [36]:

$$Y_{\lambda m_\lambda}(\hat{r}_i) h^{(1)}_\lambda(k_i r_i) = \sqrt{4\pi} \sum \begin{matrix} \lambda_1 & \lambda_2 \\ m_1 & m_2 \end{matrix} \Big| (-)^{\frac{1}{2}(\lambda+\lambda_1-\lambda_2)}$$

$$\times([\lambda_1][\lambda][\lambda_2])^{\frac{1}{2}}(\lambda_1 0,\lambda 0|\lambda_2 0)\left(\lambda_1 m_{\lambda_1},\lambda m_\lambda\,|\lambda_2 m_{\lambda_2}\right)$$

$$\times h_{\lambda_1}^{(1)}\left|\frac{m_c}{m_a+m_b}k_i r\right| j_{\lambda_2}(k_i\rho)Y_{\lambda_2 m_{\lambda_2}}(\hat{\rho})\,Y^*_{\lambda_1 m_{\lambda_1}}(\hat{r}) \quad \text{(A.18)}$$

where $[x] = 2x + 1$. Next, eqs. (A.5) and (A.6) together can be used with eq. (A.18) to put I_2 in the following form

$$I_2 = 2\pi\sqrt{4\pi}\sum\begin{Bmatrix}\lambda & \lambda_1 & \lambda_2\\ m_\lambda & m_{\lambda_1} & m_{\lambda_2}\end{Bmatrix}(-)^{\frac{1}{2}(2\lambda+\lambda_1-\lambda_2)}\eta_\lambda Y^*_{\lambda m_\lambda}(\hat{k}_1)$$

$$\times([\lambda][\lambda_1][\lambda_2])^{\frac{1}{2}}(\lambda_1 0,\lambda 0|\lambda_2 0)\left(\lambda_1 m_{\lambda_1},\lambda m_\lambda\,|\lambda_2 m_{\lambda_2}\right)$$

$$\times\left\langle e^{ik'_f\cdot\rho}e^{-ik_i\cdot r}u_\ell(\rho)\,Y_{\ell m}(\rho)\,|V_{bc}|\,U_L(r)\,Y_{LM}(\hat{r})\right.$$

$$\left.\times h^{(1)}\left(\frac{m_c}{m_c+m_b}k_i r\right)j_{\lambda_2}(k_i\rho)Y_{\lambda_2 m_{\lambda_2}}(\rho)\,Y^*_{\lambda_1 m_{\lambda_1}}(\hat{r})\right\rangle, \quad \text{(A.19)}$$

where

$$\boldsymbol{k}'_f = \frac{m_T}{m_a+m_T}\boldsymbol{k}_f\,. \quad \text{(A.20)}$$

Using the following relations

$$e^{i\boldsymbol{k}'_f\cdot\boldsymbol{\rho}} = 4\pi\sum_{\varsigma m_\varsigma}(i)^\varsigma j_\varsigma\left(k'_f\rho\right)Y^*_{\varsigma m_\varsigma}\left(\hat{k}'_f\hat{\rho}\right)Y_{\varsigma m_\varsigma},$$

$$e^{-i\boldsymbol{k}_f\cdot\boldsymbol{r}} = 4\pi\sum_{\varsigma' m_{\varsigma'}}(-i)^{\varsigma'}j_{\varsigma'}\left(k_f r\right)Y_{\varsigma' m_{\varsigma'}}\left(\hat{k}'_f\hat{\rho}\right)Y^*_{\varsigma' m_{\varsigma'}}(\hat{r}). \quad \text{(A.21)}$$

we may set:

$$I_2 = 2\pi(4\pi)^{5/2}\sum\begin{Bmatrix}\lambda & \lambda_1 & \lambda_2 & \varsigma & \varsigma'\\ m_\lambda & m_{\lambda_1} & m_{\lambda_2} & m_\varsigma & m_{\varsigma'}\end{Bmatrix}(-)^{\frac{1}{2}(2\lambda+\lambda_1-\lambda_2+\varsigma-\varsigma')}$$

$$\times\eta_\lambda Y^*_{\lambda m_\lambda}\left(\hat{k}_i\right)Y_{\varsigma m_\varsigma}\left(\hat{k}'_f\right)Y^*_{\varsigma' m_{\varsigma'}}\left(\hat{k}_f\right)([\lambda][\lambda_1][\lambda_2])^{\frac{1}{2}}(\lambda_1 0,\lambda 0|\lambda_2 0)$$

$$\times\left(\lambda_1 m_{\lambda_1},\lambda m_\lambda|\lambda_2 m_{\lambda_2}\right)\left\langle j_\varsigma\left(k'_f\rho\right)u_\ell(\rho)\,j_{\lambda_2}(k_i\rho)\right\rangle$$

$$\times\left\langle j_\varsigma\left(k_f r\right)V_{bc}(r)u_L(r)h^{(1)}_{\lambda_1}\left(\frac{m_c}{m_c+m_b}k'_i r\right)\right\rangle\int Y^*_{\varsigma m_\varsigma}(\hat{\rho})\,Y^*_{\ell m}(\hat{\rho})$$

$$\times Y_{\lambda_2 m_{\lambda_2}}(\hat{\rho})\,d\,\Omega_\rho\int Y_{\varsigma' m_{\varsigma'}}(\hat{r})\,Y_{LM}(\hat{r})Y_{\lambda_1 m_{\lambda_1}}(\hat{r})\,d\,\Omega_r\,. \quad \text{(A.22)}$$

By taking k_f as an axis of quantization as shown in Figure 2(a), and knowing that [36]

$$Y^*_{\varsigma' m_{\varsigma'}}\left(\hat{k}_f\right) = Y^*_{\varsigma' m_{\varsigma'}}(0,\Phi) = \delta_{\varsigma' 0}\sqrt{\frac{[\varsigma']}{4\pi}}\,, \quad \text{(A.23)}$$

we deduce that $m_{\varsigma'} = 0$; further,

$$Y^*_{\varsigma m_\varsigma}\left(\hat{k}'_f\right) = Y^*_{\varsigma m_\varsigma}(0,\Phi) = \delta_{\varsigma 0}, \quad \text{(A.24)}$$

implies that $m_{\varsigma'} = 0$. Therefore, I_2 becomes

$$I_2 = 2\pi(4\pi)^{3/2}\sum\begin{Bmatrix}\lambda & \lambda_1 & \lambda_2 & \varsigma & \varsigma'\\ m_\lambda & m_{\lambda_1} & m_{\lambda_2} & & \end{Bmatrix}(-)^{\frac{1}{2}(2\lambda+\lambda_1-\lambda_2+\varsigma-\varsigma')}$$

$$\times Y^*_{\lambda m_\lambda}\left(\hat{k}_i\right)([\lambda_1][\lambda_2][\lambda][\varsigma][\varsigma'])^{\frac{1}{2}}(\lambda_1 0,\lambda 0|\lambda_2 0)$$

$$\times\left(\lambda_1 m_{\lambda_1},\lambda m_\lambda|\lambda_2 m_{\lambda_2}\right)\int Y^*_{\varsigma 0}(\hat{\rho})\,Y^*_{\ell m}(\hat{\rho})\,Y_{\lambda_2 m_{\lambda_2}}(\hat{\rho})\,d\,\Omega_\rho$$

$$\int Y^*_{\varsigma' 0}(\hat{r})\,Y_{LM}(\hat{r})Y_{\lambda_1 m_{\lambda_1}}(\hat{r})\,d\,\Omega_r\tau_2\,. \quad \text{(A.}$$

where τ_2 is given by

$$\tau_2 = \left\langle j_{\varsigma'}\left(k_f r\right)V_{bc}(r)u_L(r)\,h^{(1)}_{\lambda_1}\left(\frac{m_c}{m_a+m_b}k_i\right.\right.$$

$$\left.\left\langle j_\varsigma\left(k'_f\rho\right)u_\ell(\rho)\,j_{\lambda_2}(k_i\rho)\right\rangle\right.\Big\rangle.$$

Now, we shall use the following relations for the spherical harmonics [36]:

$$\int Y_{\ell_1 m_1}(\hat{r})\,Y_{\ell_2 m_2}(\hat{r})\,Y^*_{\ell m}(\hat{r})\,d\Omega_r = \left(\frac{[\ell_1][\ell_2]}{4\pi[\ell]}\right)^{\frac{1}{2}}(\ell_1 0,\ell_2 0|\ell 0)$$

$$\times\left(\ell_1 m_1,\ell_2 m_2|\ell m\right),$$

$$m_1+m_2 = m,\ |\ell_1-\ell|\le\ell_2\le|\ell_1-\ell_2|, \quad \text{(A.2}$$

$$\int Y^*_{\varsigma 0}(\rho)\,Y^*_{\ell m}(\rho)Y_{\lambda_2 m_{\lambda_2}}(\rho) = (-)^m Y^*_{\ell,-m}(\hat{\rho})\,Y_{\lambda_2 m_{\lambda_2}}(\hat{\rho})Y^*_{\varsigma 0}(\rho)d\Omega_\rho$$

$$= (-)^m\left(\frac{[\ell][\lambda_2]}{4\pi[\varsigma]}\right)^{\frac{1}{2}}(\ell 0,\lambda_2 0|\varsigma 0)\left(\ell-m,\lambda_2 m|\varsigma 0\right) \quad \text{(A.2}$$

and

$$\int Y^*_{\varsigma' 0}(\hat{r})\,Y_{LM}(\hat{r})\,Y_{\lambda_1 m_{\lambda_1}}(\hat{r})\,d\Omega_r$$

$$= (-)^{m\lambda_1}\int Y_{LM}(\hat{r})\,Y_{\lambda_1,-m_{\lambda_1}}(\hat{r})\,Y^*_{\varsigma'}(\hat{r})\,d\Omega_r$$

$$= (-)^M\left(\frac{[L][\lambda_2]}{4\pi[\varsigma']}\right)^{\frac{1}{2}}(L0,\lambda_1 0|\varsigma' 0)(LM,\lambda_1-M|\varsigma' 0) \quad \text{(A.2}$$

in eq. (A.25) to get:

$$I_2 = 2\pi\sqrt{4\pi}\sum\begin{Bmatrix}\lambda & \lambda_1 & \lambda_2 & \varsigma & \varsigma'\\ m_\lambda & m & M & & \end{Bmatrix}(-)^{m+M}(-)^{\frac{1}{2}(2\lambda+\lambda_1-\lambda_2+\varsigma-\varsigma')}$$

$$\times\eta_\lambda Y_{\lambda m_\lambda}(\hat{k}_i)\left([\lambda_2]^2[\lambda_1]^2[\lambda][L][\ell]\right)^{\frac{1}{2}}(\lambda_1 0,\lambda 0|\lambda_2 0)$$

$$\times(\lambda_1 M,\lambda m_\lambda|\lambda_2 m)(L0,\lambda_1 0|\varsigma' 0)(LM,\lambda_1-M|\varsigma' 0)$$

$$\times(\ell 0,\lambda_2 0|\varsigma 0)(\ell-m,\lambda_2 m|\varsigma 0)\times\tau_2. \qquad (A.30)$$

The summation over ς' may be evaluated by making use of the asymptotic form of the Clebsch-Gordan coefficients [36] with two large values of the angular momentum and one small value, one may write

$$(\ell_1,\ell_2-Z;m_2-m_1|\ell_2 m_2)=(-)^{\ell_1-Z}P^{\ell_1}_{m_1 Z}\left(\cos^{-1}\frac{m_2}{\ell_2}\right), \qquad (A.31)$$

where Z is very small value of angular momentum and D is the rotation matrix. Then one may write for the sum over ς' in (A.30) the following expression:

$$\sum_{\varsigma'}(-)^{\frac{1}{2}(\lambda_1-\varsigma')}(L0,\lambda_1 0|\varsigma' 0)(LM,\lambda_1-M|\varsigma' 0)$$

$$=\sum_{\varsigma'}(-)^{\varsigma'-Z/2}(L0,\varsigma'-Z;0|\varsigma' 0)(LM,\varsigma'-Z;-M|\varsigma' 0)$$

$$=\sum_Z(i)^{-Z}(-)^{L-Z}D^L_{0Z}\left(\frac{\pi}{2}\right)(-)^{L-Z}D^L_{MZ}\left(\frac{\pi}{2}\right.$$

$$=\sum_Z(i)^{-Z}D^L_{0Z}\left(\frac{\pi}{2}\right)D^L_{MZ}\left(\frac{\pi}{2}\right. \qquad (A.32)$$

using the relation [36]

$$D^J_{MK}(\beta)=(-)^{M-k}D^J_{KM}(\beta),$$

$$D^J_{MK}(\alpha,\beta,\gamma)=e^{-iM\alpha}D^J_{KM}(\beta)\,e^{-ik\gamma}, \qquad (A.33)$$

we get for eq. (A.32)

$$\sum_Z(i)^{-Z}D^L_{MZ}\left(\frac{\pi}{2}\right)(-)^{-Z}D^L_{Z0}\left(\frac{\pi}{2}\right)=\sum_Z(i)^{-3Z}D^L_{MZ}\left(\frac{\pi}{2}\right)D^L_{Z0}\left(\frac{\pi}{2}\right.$$

$$=\sum_Z e^{-\frac{i3\pi Z}{2}}D^L_{MZ}\left(\frac{\pi}{2}\right)D^L_{Z0}\left(\frac{\pi}{2}\right)$$

$$=\sum_Z D^L_{MZ}\left(0,\frac{\pi}{2},0\right)D^L_{Z0}\left(\frac{3\pi}{2},\frac{\pi}{2},0\right). \qquad (A.34)$$

Now by making use of the relations [36]

$$\sum_{m'}D^\ell_{mm'}(\alpha_2\,\beta_2\,\gamma_2)\,D^\ell_{m'm''}(\alpha_1\,\beta_1\,\gamma_1)=D^\ell_{m'm''}(\alpha_3\,\beta_3\,\gamma_3),$$

$$\cos\beta_3=\cos\beta_1\cos\beta_2-\sin\beta_1\sin\beta_2\cos\delta_2,$$

$$\frac{\sin\beta_i}{\sin\delta_i}=\frac{\sin\beta_j}{\sin\delta_j},$$

$$\delta_1=\alpha_2-\alpha_3+\pi,\ \delta_2=\gamma_1-\gamma_3-\pi\ \ \delta_3=\alpha_1+\gamma_2. \qquad (A.35)$$

eq. (A.34) can be rewritten as:

$$\sum_Z D^L_{MZ}\left(0,\frac{\pi}{2},0\right)D^L_{Z0}\left(\frac{3\pi}{2},\frac{\pi}{2},0\right)=D^L_{M0}\left(\frac{\pi}{2},\frac{\pi}{2},\frac{\pi}{2}\right)$$

$$\sqrt{\frac{4\pi}{[L]}}\,Y^*_{LM}\left(\frac{\pi}{2},-\frac{\pi}{2}\right), \qquad (A.36)$$

where the following relation have been used

$$D^{*\ell}_{m0}(\alpha,\beta,\gamma)=\sqrt{\frac{4\pi}{[\ell]}}\,Y_{\ell m}(\beta,\alpha). \qquad (A.37)$$

In doing the summation, we have assumed $\varsigma''-\lambda_1=Z$ and $[\varsigma'']=[\lambda_1]$ for small Z. Now, consider the summation over ς: Assume that $\varsigma-\lambda_2=Z$ and $[\varsigma]=[\lambda_2]$ for small Z; we then get:

$$\sum(-)^{\frac{1}{2}(\varsigma-\lambda_2'')}(\ell 0,\lambda_2 0|\varsigma 0)(\ell-m,\lambda_2 m|\varsigma 0) \qquad (A.38)$$

$$=\sum(-)^{\frac{1}{2}(\varsigma-\lambda_2)}(\ell 0,\varsigma-Z,0|\varsigma 0)(\ell-m,\varsigma-Z;m|\varsigma 0)$$

$$=\sum_Z(i)^Z(i)^{\ell-Z}D^\ell_{0Z}\left(\frac{\pi}{2}\right)(-)^{\ell-Z}D^\ell_{-mZ}\left(\frac{\pi}{2}\right.$$

$$=\sum_Z(i)^Z D^\ell_{0Z}\left(\frac{\pi}{2}\right)D^\ell_{-mZ}\left(\frac{\pi}{2}\right). \qquad (A.39)$$

By using eqs. (A.33), (A.35) and (A.37), we get

$$\sum(i)^Z(i)^Z D^\ell_{-mZ}\left(\frac{\pi}{2}\right)D^\ell_{Z0}\left(\frac{\pi}{2}\right)=\sum_Z e^{\frac{i\pi Z}{2}}D^\ell_{-mZ}\left(\frac{\pi}{2}\right)D^\ell_{Z0}\left(\frac{\pi}{2}\right.$$

$$=(-)^m\sqrt{\frac{4\pi}{[\ell]}}Y_{\ell m}\left(\frac{\pi}{2},\frac{\pi}{2}\right). \qquad (A.40)$$

Substituting eqs. (A.37) and (A.40) into eq. (A.30), we get:

$$I_2=2\pi(4\pi)^{\frac{3}{2}}\sum\begin{Bmatrix}\lambda & \lambda_1 & \lambda_2\\ m_\lambda & m & M\end{Bmatrix}(-)^m(-)^\lambda[\lambda_1][\lambda_2][\lambda]^{\frac{1}{2}}$$

$$\times \eta_\lambda Y^*_{\lambda m_\lambda}(\hat{k}_t)\, Y^*_{LM}\left(\frac{\pi}{2},\frac{\pi}{2}\right) Y_{\ell m}\left(\frac{\pi}{2},\frac{\pi}{2}\right)(\lambda_1 0, \lambda\, 0\,|\lambda_2 0)$$

$$(\lambda_1 M, \lambda m_\lambda|\lambda_2 m)\times\tau_2 . \qquad (A.41)$$

Adopting the same method for calculating the sum over λ_1 and λ_2, we get

$$\sum_{\lambda_1}(\lambda_1 0, \lambda\, 0\,|\lambda_2 0)\,(\lambda_1 M, \lambda m_\lambda|\lambda_2 m)$$

$$= \sum_{\lambda_1}(-)^{m+M}\frac{[\lambda_2]}{[\lambda_1]}(\lambda 0, \lambda_2 0|\lambda_1 0)(\lambda m_\lambda, \lambda_2 - m|\lambda_1 - M) \qquad (A.42)$$

$$= \sum_{\lambda_1}(-)^{m+M'}\frac{[\lambda_2]}{[\lambda_1]}(\lambda 0, \lambda_1 - Z0|\lambda_1 0)(\lambda m_\lambda, \lambda_1 - Z; -m|\lambda_1 - M)$$

$$= (-)^{2M}\frac{[\lambda_2]}{[\lambda_1]}\sum_\gamma D^\lambda_{m_\lambda Z}(-\pi,0,0)\, D^\lambda_{Z0}\left(\pi,\frac{\pi}{2},0\right). \qquad (A.43)$$

By using eq. (A.35), eq. (A.43) becomes

$$(-)^{2M}\frac{[\lambda_2]}{[\lambda_1]} D^\lambda_{m_\lambda 0}\left(0,\frac{\pi}{2},-\theta,-\pi\right)$$

$$= (-)^{2M}\frac{[\lambda_2]}{[\lambda_1]}\sqrt{\frac{4\pi}{[\lambda]}}Y_{\lambda m_\lambda}\left(\frac{\pi}{2},-\theta,0\right), \qquad (A.44)$$

where

$$\theta = \cos^{-1}\left|\frac{M}{\lambda}\right|. \qquad (A.45)$$

By using eq. (A.44), one can write eq. (A.41) in the following form:

$$I_2 = (8\pi^2)\sum\begin{Bmatrix}\lambda & \ell & L\\ m & M & \end{Bmatrix}(-)^{2M+m}(-)^\lambda[\lambda]^3\eta_\lambda P_\lambda(\mu)$$

$$\times Y_{\ell -m}\left(\frac{\pi}{2},\frac{\pi}{2}\right)Y^*_{L-M}\left(\frac{\pi}{2},-\frac{\pi}{2}\right)\times\tau_2 , \qquad (A.46)$$

where $\mu = \cos\vartheta$ and ϑ is the angle between $\boldsymbol{k}_i$ and the vector of polar angles $(\pi/2-\theta)$ and 0^0. In writing eq. (A.46), we have used addition theorem for spherical harmonics [23]:

$$\frac{[\ell]}{4\pi}P_\ell(\cos\vartheta) = \sum Y^*_{\ell m}(\vartheta',\Phi')\,Y_{\ell m}(\vartheta'',\varphi''),$$

$$\cos\vartheta = \cos\vartheta'\cos\vartheta'' + \sin\vartheta'\sin\vartheta''\cos(\varphi''-\varphi'). \qquad (A.47)$$

A practical method to carry out the summation over λ in eq. (A.46), based on the use of the Watson-Sommerfeld transformation [24], permits us to transform the summation over λ into a contour integration in the corresponding complex plane. According to this approach, the sum over λ in eq. (A.46) can be transformed into an integral form as [37]:

$$\sum_\lambda(-)^\lambda[\lambda]^3\eta_\lambda\, P_\lambda(\mu) = \frac{1}{2\ell}\int_{C_1}\frac{[\lambda]^3}{\sin(\lambda\pi)}\eta_\lambda\, P_\lambda(-\mu)\,d\lambda \qquad (A.48)$$

Here λ represents a complex angular momentum. The path of integration C1 is shown in Figure 2 (b). In the Regge pole representation, eq. (A.48) reduces to a sum over Regge-poles in the following manner

$$\sum_\lambda(-)^\lambda[\lambda]^3\eta_\lambda\, P_\lambda(\mu) = \pi\sum_n\frac{[\lambda_n]^3 R_{\lambda_n}P_{\lambda_n}(-\mu)}{\sin(\lambda_n\pi)} \qquad (A.49)$$

Here, λ_n is the position of the nth pole and $R_{\lambda n}$ is the residue of the scattering coefficient η_λ at the pole n. By introducing the Wood-Saxon form for η_λ

$$\eta_\lambda = \frac{\cdot}{1+e^{\left(\frac{\lambda-\lambda_0}{\Delta}\right)}}, \qquad (A.50)$$

the nth pole position is determined using

$$\lambda_n = \lambda_0 + in\pi\Delta, \quad (n = \pm 1, \pm 3, \pm 5, \ldots\ldots). \qquad (A.51)$$

The residues of η_λ are all equal to Δ. In order to simplify (A.49), the following approximation is being used [37]

$$\frac{P_\lambda(-\mu)}{\sin(\lambda\pi)} = -i\varsigma\frac{\sqrt{2}}{\sqrt{\pi\lambda\sin\vartheta}}e^{i\varsigma\left[\left(R_e\lambda+\frac{1}{2}\right)\vartheta-\frac{\pi}{4}\right]-|I_m\lambda|\vartheta}, \qquad (A.52)$$

where $\dfrac{I_m\lambda}{|I_m\lambda|} = \pm 1$.

Thus, eq. (A.49) becomes

$$\sum(-)^\lambda(2\lambda+1)^3\eta_\lambda P_\lambda(\mu) = \pi\Delta\sum(2\lambda_n+1)^3$$

$$\times\sqrt{\frac{2}{\pi\lambda_n\sin\vartheta}}(-i\varsigma)e^{i\varsigma\left[\left(\lambda_0+\frac{1}{2}\right)\vartheta-\frac{\pi}{4}\right]-|n\pi\Delta|\vartheta} \qquad (A.53)$$

If we consider only the poles corresponding to $n = \pm$ where n is the integer appearing in eq. (A.51), then the right hand side of eq. (A.53) can be rewritten as:

$$\pi\Delta\,(2\lambda_1+1)^3\sqrt{\frac{2}{\pi\lambda_1\sin\vartheta}}(-i)e^{i\left[\left(\lambda_0+\frac{1}{2}\right)\vartheta-\frac{\pi}{4}\right]-\pi\Delta\vartheta}$$

$$+(l)(2\lambda_{-1}+1)^3\sqrt{\frac{}{\pi\lambda_{-1}\sin\vartheta}}\;e^{-i\left[\left(\lambda_0+\frac{1}{2}\right)\vartheta-\frac{\pi}{4}\right]-\pi\Delta\vartheta}. \quad \text{(A.54)}$$

$\lambda_0 > 1$, and $\lambda_0 >> \Delta$, the following approximation can be used

$$[\lambda_1] = 2\lambda_1 + 1 \cong 2\lambda_1 \cong \frac{1}{2\lambda_0}\left(4\lambda_0^2 + 2\pi^2\Delta^2\right)e^{\frac{i\pi\pi}{\lambda_0}}. \quad \text{(A.55)}$$

Substituting eqs. (A.54) and (A.55) into eq. (A.46) we get:

$$I_2 = 32\pi^2\Delta\sum\begin{Bmatrix}\ell & L\\ m & M\end{Bmatrix}(-1)^{2M+m}Y_{\ell m}\left\{\frac{\pi}{2},\frac{\pi}{2}\right\}Y^*_{L-M}\left\{\frac{\pi}{2},\frac{\pi}{2}\right\}$$

$$\frac{\left[4\lambda_0^2+2\pi^2\Delta^2\right]^{\frac{5}{2}}}{(2\lambda_0)^{\frac{5}{2}}\sqrt{\sin\vartheta}}\sin\left[\left(\lambda_0+\frac{1}{2}\right)\vartheta-\frac{\pi}{4}+\frac{5\pi\Delta}{2\lambda_0}\right]e^{\pi\Delta\vartheta}\times\tau_2. \quad \text{(A.56)}$$

If the projectile is in a relative S-state, then $L = M = 0$; which gives a value of $\pi/2$ for the angle ϑ (the scattering angle) between $\boldsymbol{k}_i$ and $\boldsymbol{k}_f$ and the radial integral τ_2, eq. (A.25), can be evaluated at the points defined by

$$\varsigma = \lambda_2 = \ell_0 \cong kR, \text{ and } \varsigma' = \lambda_1 = \ell_0 \cong kR, \quad \text{(A.57)}$$

where ℓ_0 is the grazing angular momentum, and R is the interaction radius.

This approximation is quite accurate for strongly absorbed particles at medium and high energies if $|\varsigma - \lambda_2|$ and $|\varsigma' - \lambda_1|$ are not too large. The main basis for its validity is the fact that in strong absorption situations, the DWBA radial integrals are sharply localized in the angular-momentum space in the vicinity of the cut-off angular momentum ℓ_0 [38-40].

Now, the total bound state Morinigo wave functions are defined by [32,35]

$$\Phi_\ell^m(r) = A_\ell Y_{\ell m}(\Omega)\, r^{\ell}\cdot^{\nu}e^{-\beta_\ell r} \quad \text{(A.58)}$$

Using the Morinigo form given in the above equation for the wave function $u_\ell(\rho)$, then the first integral of τ_2 can be written as:

$$\int j_\varsigma\left(k_f'\rho\right)u_\ell(\rho)j_{\lambda_2}(k_i\rho)\rho^2 d\rho$$

$$= N_\ell j_{\ell 0}\left(k_f' R_{\ell T}\right)j_{\ell 0}\left(k_i R_{\ell T}\right)\int e^{-\gamma\rho}\rho^{\ell-1}\rho^2 d\rho$$

$$= N_\ell j_{\ell 0}\left(k_f' R_{\ell T}\right)j_{\ell 0}\left(k_i R_{\ell T}\right)\frac{\Gamma(\ell+2)}{\gamma^{\ell+2}}, \quad \text{(A.59)}$$

where $R_{\ell I}$ is the interaction parameter given by [38]:

$$R_{\ell I} = r_0\left[A_\ell^{1/3} + A_T^{1/3}\right]. \quad \text{(A.60)}$$

Here, A is the mass number.

In obtaining eq (A.59), we have considered the oscillatory functions outside the integral at $\rho = R_{\ell I}$ [12]. Following the same procedures, considering the Hulthen form for $V_{b_\ell}(r)$ as in eq. (A.15) and taking the form of the wave function $u_0(r)$ to be:

$$u_0(r) = e^{\gamma r}\left(1 - e^{-r/a}\right), \text{ in the interior region,}$$
$$= e^{-\gamma r}, \text{ in the asymptotic region,} \quad \text{(A.61)}$$

the second integral of τ_2 can be written as:

$$\int j_{\varsigma'}\left(k_f r\right)V_{b_\ell}(r)u_I(r)h^{(1)}_{\lambda_1}\left(\frac{m_\ell}{m_\ell + m}k_i r\right)r^2 dr$$

$$\frac{N_0 V_0}{\beta^2}j_{\ell 0}\left(k_f R_{b_\ell}\right)h\left(\frac{m_\ell}{m_\ell + m_b}k_i R_{b_\ell}\right), \quad \text{(A.62)}$$

where γ is the radius of the projectile particle and a is the nuclear potential range. Using eqs. (A.59) and (A.62), the second integral of τ_2 can be written as:

$$\tau_2 = N_0 V_0 N_\ell \frac{\Gamma(\ell+2)}{\beta^2\gamma^{\ell+2}}j_{\ell 0}\left(k_f' R_{\ell T}\right)J_{\ell 0}\left(k_i R_{\ell T}\right)$$

$$\times j_{\ell 0}\left(k_f R_{b_\ell}\right)j^{(1)}_{\ell 0}\left(\frac{m_\ell}{m_\ell + m_b}k_i R_{b_\ell}\right) \quad \text{(A.63)}$$

Substituting eq. (A.63) into (A.56), we obtain:

$$I_2 = 16\pi^2\Delta\sum_{\ell m}(-1)^m N_0 V_0 N_\ell \frac{\Gamma(\ell+2)}{\beta^2\gamma^{\ell+2}}j_{\ell 0}\left(k_f' R_{\ell T}\right)$$

$$\times J_{\ell 0}\left(k_i R_{\ell T}\right)j_{\ell 0}\left(k_f R_{b_\ell}\right)h^{(1)}_{\ell 0}\left(\frac{m_\ell}{m_\ell + m_b}k_i R_{b_\ell}\right)$$

$$\times\frac{\left(4\lambda_0^2+2\pi^2\Delta^2\right)^{5/2}}{(2\lambda_0)^{5/2}\sqrt{\sin\vartheta}}\sin\left[\left(\lambda_0+\frac{1}{2}\right)\vartheta-\frac{\pi}{4}+\frac{5\pi\pi}{2\lambda_0}\right]e^{-\pi\Delta\vartheta} \quad \text{(A.64)}$$

Using the expressions of I_1 and I_2 that are given by eqs. (A.17) and (A.64), the angular distribution can be put into its final form of eq. (24).